Research Article Vol. 25, No. 3 | 6 Feb 2017 | OPTICS EXPRESS 2206

Optics EXPRESS

Broadband instantaneous frequency measurement based on stimulated Brillouin scattering

XIN LONG, WEIWEN ZOU,* AND JIANPING CHEN

State Key Laboratory of Advanced Optical Communication Systems and Networks, Department of Electronic Engineering, Shanghai Jiao Tong University, Shanghai 200240, China

*wzou@sjtu.edu.cn

Abstract: A technique for the instantaneous frequency measurement (IFM) of broadband signals is proposed based on stimulated Brillouin scattering (SBS) in a single-mode optical fiber. The instantaneous frequency and amplitude information is obtained by the narrowband filtering of the acoustic-optic interaction in the SBS process. Through sideband management of the optical-modulation, the IFM bandwidth can be far beyond the Brillouin frequency shift (i.e. ~11 GHz in 1550 nm). Proof-of-concept experiments for both the linearly frequency modulated pulse and frequency Costas coded pulse are carried out to verify the feasibility of the IFM.

OCIS codes: (070.4790) Spectrum analysis; (190.0190) Nonlinear optics; (290.5900) Scattering, stimulated Brillouin.

References and links

1. S. Pan and J. Yao, "Photonics-based broadband microwave measurement," J. Lightwave Technol. in press).
2. J. Capmany and D. Novak, "Microwave photonics combines two worlds," Nat. Photonics **1**(6), 319–330 (2007).
3. J. Yao, "Microwave photonics," J. Lightwave Technol. **27**(3), 314–335 (2009).
4. P. Ghelfi, F. Laghezza, F. Scotti, G. Serafino, A. Capria, S. Pinna, D. Onori, C. Porzi, M. Scaffardi, A. Malacarne, V. Vercesi, E. Lazzeri, F. Berizzi, and A. Bogoni, "A fully photonics-based coherent radar system," Nature **507**(7492), 341–345 (2014).
5. W. Zou, H. Zhang, X. Long, S. Zhang, Y. Cui, and J. Chen, "All-optical central-frequency-programmable and bandwidth-tailorable radar," Sci. Rep. **6**, 19786 (2016).
6. L. V. T. Nguyen and D. B. Hunter, "A photonic technique for microwave frequency measurement," IEEE Photonics Technol. Lett. **18**(9), 1188–1190 (2006).
7. H. Emami, N. Sarkhosh, L. A. Bui, and A. Mitchell, "Wideband RF photonic in-phase and quadrature-phase generation," Opt. Lett. **33**(2), 98–100 (2008).
8. J. Zhou, S. Fu, S. Aditya, P. P. Shum, and C. Lin, "Instantaneous microwave frequency measurement using photonic technique," IEEE Photonics Technol. Lett. **21**(15), 1069–1071 (2009).
9. Z. Li, C. Wang, M. Li, H. Chi, X. Zhang, and J. Yao, "Instantaneous microwave frequency measurement using a special fiber Bragg grating," IEEE Microw. Wireless Commun. **21**(1), 52–54 (2011).
10. M. Pagani, B. Morrison, Y. Zhang, A. Casas-Bedoya, T. Aalto, M. Harjanne, M. Kapulainen, B. J. Eggleton, and D. Marpaung, "Low-error and broadband microwave frequency measurement in a silicon chip," Optica **2**(8), 751–756 (2015).
11. D. Marpaung, "On-chip photonic-assisted instantaneous microwave frequency measurement system," IEEE Photonics Technol. Lett. **25**(9), 837–840 (2013).
12. J. Niu, S. Fu, K. Xu, J. Zhou, S. Aditya, J. Wu, P. P. Shum, and J. T. Lin, "Instantaneous microwave frequency measurement based on amplified fiber-optic recirculating delay loop and broadband incoherent light source," J. Lightwave Technol. **29**(1), 78–84 (2011).
13. T. A. Nguyen, E. H. W. Chan, and R. A. Minasian, "Instantaneous high-resolution multiple-frequency measurement system based on frequency-to-time mapping technique," Opt. Lett. **39**(8), 2419–2422 (2014).
14. D. Lam, B. W. Buckley, C. K. Lonappan, A. M. Madni, and B. Jalali, "Ultra-wideband instantaneous frequency estimation," IEEE Instrum. Meas. Mag. **18**(2), 26–30 (2015).
15. G. P. Agrawal, *Nonlinear Fiber Optics* (Academic Press, 2007).
16. T. Tanemura, Y. Takushima, and K. Kikuchi, "Narrowband optical filter, with a variable transmission spectrum, using stimulated Brillouin scattering in optical fiber," Opt. Lett. **27**(17), 1552–1554 (2002).
17. B. Vidal, M. A. Piqueras, and J. Martí, "Tunable and reconfigurable photonic microwave filter based on stimulated Brillouin scattering," Opt. Lett. **32**(1), 23–25 (2007).

#281556 https://doi.org/10.1364/OE.25.002206
Journal © 2017 Received 24 Nov 2016; revised 19 Jan 2017; accepted 20 Jan 2017; published 26 Jan 2017

18. D. Marpaung, B. Morrison, M. Pagani, D. Y. Choi, B. Luther-Davies, S. J. Madden, and B. J. Eggleton, "Low power, chip-based stimulated Brillouin scattering microwave photonic filter with ultrahigh selectivity," Optica **2**(2), 76–83 (2015).
19. W. Zhang and R. A. Minasian, "Widely tunable single-passband microwave photonic filter based on stimulated Brillouin scattering," IEEE Photonics Technol. Lett. **23**(23), 1775–1777 (2011).
20. H. Jiang, D. Marpaung, M. Pagani, K. Vu, D.-Y. Choi, S. J. Madden, L. Yan, and B. J. Eggleton, "Wide-range, high-precision multiple microwave frequency measurement using a chip-based photonic Brillouin filter," Optica **3**(1), 30–34 (2016).
21. S. Shakthi, A. Suresh, V. Reddy, and R. Pant, "Wideband instantaneous frequency measurement using stimulated Brillouin scattering," in *Photonics and Fiber Technology Congress* (2016), paper AT5C.5.
22. W. Li, N. H. Zhu, and L. X. Wang, "Brillouin-assisted microwave frequency measurement with adjustable measurement range and resolution," Opt. Lett. **37**(2), 166–168 (2012).
23. X. Long, W. Zou, H. Li, and J. Chen, "Critical condition for spectrum distortion of pump–probe-based stimulated Brillouin scattering in an optical fiber," Appl. Phys. Express **7**(8), 082501 (2014).
24. M. C. Li, "A high precision Doppler radar based on optical fiber delay loops," IEEE Trans. Antenn. Propag. **52**(12), 3319–3328 (2004).
25. A. L. Gaeta and R. W. Boyd, "Stochastic dynamics of stimulated Brillouin scattering in an optical fiber," Phys. Rev. A **44**(5), 3205–3209 (1991).
26. W. Zou, Z. He, and K. Hotate, "Experimental study of Brillouin scattering in fluorine-doped single-mode optical fibers," Opt. Express **16**(23), 18804–18812 (2008).
27. N. Levanon and E. Mozeson, *Radar Signals* (Wiley, 2004).

1. Introduction

Characterization of an unknown microwave signal is important in high speed communications, radar detection, and space exploration fields, etc. Among them, the spectrum analysis and instantaneous frequency measurement (IFM) are widely used in radar warning receivers, anti-stealth defense, and electronic intelligence systems. Compared to the signal source analyzer, the IFM technique is able to determine the instantaneous frequency (i.e. spectrum changing with time) of an unknown signal with the use of low-cost and low-speed photodetectors instead of expensive electronic receivers. Besides, the IFM technique is of importance for RF design and characterization. Traditional measurements implemented by electronic devices keep the advantages of high resolution and flexibility. However, when characterizing broadband signals beyond tens of gigahertz, electronic systems suffer difficulty and complexity [1]. On the other hand, the emerging microwave photonics technique provides a promising and reliable solution in generation, control, and processing of the broadband microwave signals [2–5]. The photonic technique is potentially helpful to reduce the size, weight, power, and cost of the whole system with the development of integrated photonics. In recent years, several microwave photonics schemes based on the frequency-to-power or frequency-to-time mapping have been proposed to implement the IFM for unknown microwave signals [6–11]. More recently, several works have been done for high resolution and the ability to deal with multiple tones [12–14].

In optical fibers, stimulated Brillouin scattering (SBS) process is a nonlinear phenomenon of three-wave interaction involving the pump lightwave, counter-propagating probe lightwave, and acoustic wave [15]. The Brillouin gain is dependent on the frequency difference between these two lightwaves and reaches the maximum value when the frequency difference equals the Brillouin frequency shift (BFS) of an optical fiber. This frequency selectivity enables the SBS process to pursue high quality microwave photonic filtering [16–19]. With the help of the filtering nature, several SBS based IFM schemes have been proposed [20–22]. The work in [21] relies on the dependence of the BFS on the optical wavelength, which makes it difficult to precisely determine the signal with low frequency. Li *et al* has realized a SBS based scheme with adjustable measurement range and resolution [22] whereas it didn't demonstrate high spectral resolution and wide bandwidth simultaneously. Moreover, the frequency of the signal to be detected in these schemes should be constant or composed of several tones.

In this work, we present a flexible and simple broadband IFM scheme based on the SBS in a standard single-mode optical fiber. Unlike the work in [20–22], this scheme can detect

Optics EXPRESS

more types of signals instead of single-tone or multi-tone signals. Moreover, the instantaneous spectrum information (i.e. frequency changing with time) of this scheme can be determined and quantified. The experimental system is based on a pump-probe configuration and the IFM is performed by modulating the signal to be detected onto the probe lightwave and tuning the frequency of the counter-propagating pump lightwave. In principle, the instantaneous information (including both frequency and power) is extracted by the SBS process and obtained through detecting the Brillouin gain of the probe lightwave. According to the theoretical analysis, the spectral resolution is decided by the linewidth of Brillouin gain spectrum (BGS) and the temporal resolution is dependent on the phonon lifetime (~10 ns in an optical fiber). Through selecting the sidebands of the electro-optic modulator, the IFM bandwidth goes essentially beyond the BFS of ~11 GHz in 1550 nm and is limited only by the bandwidth of the modulator used in this study. In the experiment, linearly frequency modulated (LFM) pulse and frequency Costas coded pulse are selected as the signals to be processed. The measured frequency errors are within 20 MHz and the broadband LFM of more than 27 GHz is realized.

2. Principle

The SBS process has been widely adopted as a microwave photonic filtering due to its narrow linewidth. In particular, for a pump-probe based configuration with single-frequency continuous wave (CW) pump lightwave injected, the detected probe gain is the filtered component of the injected probe lightwave, which is given by

$$E_{Sout}\left(t+T\right)-E_{S0}\left(t\right)\propto LF^{-1}\left[\frac{\boldsymbol{E}_{S0}\left(\omega\right)}{1/\left(2\tau_p\right)+i\left(\omega-\omega_L+\omega_B\right)}\right], \quad (1)$$

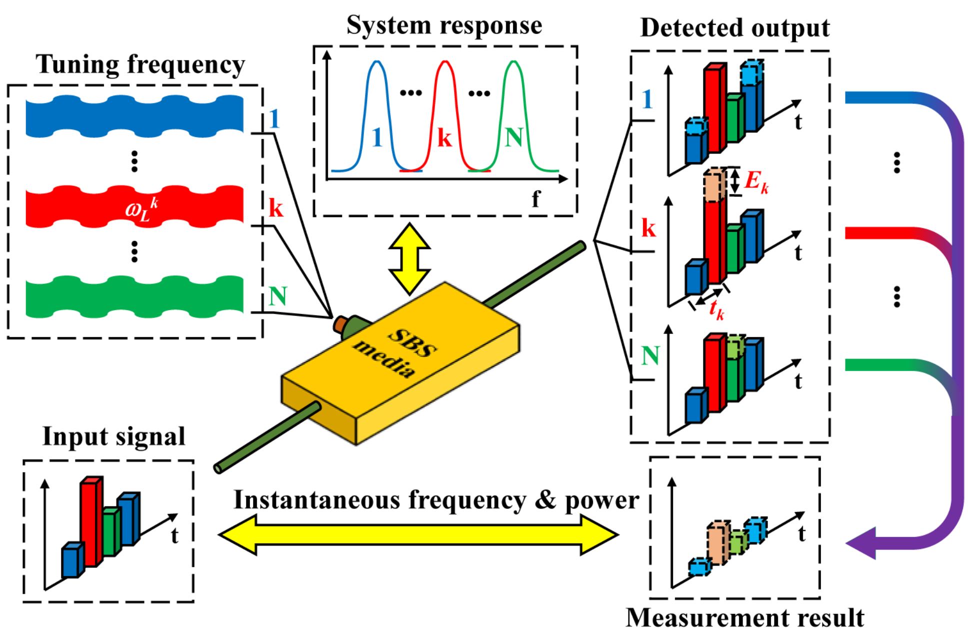

Fig. 1. Principle of the broadband IFM based on SBS process. The center of the filtering response is selected by tuning the frequency of the pump lightwave. After the SBS media (such as an optical fiber), the corresponding frequency component of the probe lightwave is scanned and amplified. The combined measurement result reveals the instantaneous frequency and power information of the signal that is modulated on the probe lightwave.

where E_{S0} and E_{Sout} represents the slowly-varying envelopes of launched and detected probe lightwaves, respectively. L is the fiber length and T is the time for lightwave to pass through the fiber. F^{-1} is the inverse Fourier transformation. τ_p stands for the phonon lifetime. ω_L is the pump frequency and ω_B is the BFS of the optical fiber.

The principle of the proposed IFM is schematically illustrated in Fig. 1. The Brillouin filter expressed in Eq. (1) is described by τ_p and ω_L - ω_B, determining the spectral resolution and center of this filter, respectively. The whole measurement includes multiple repeated steps. In the k-th step measurement, ω_L of the pump wave is set to be ω_L^k, which provides a Brillouin filter at the frequency center of ω_L^k-ω_B. Through the SBS process, the corresponding component of the input signal is amplified at the temporal position of t_k. The measured probe gain E_k is proportional to the amplitude of the input signal due to the same pump power. The pump depletion in the SBS process will distort this relation and it is avoided by controlling the pump/probe power and the fiber length [23]. For each step measurement, the relation among time, frequency, and amplitude (t_k, ω_L^k-ω_B, and E_k) is determined. In the next-step measurement, ω_L is tuned to another frequency to detect another time-frequency-amplitude relation. After the repeated steps, the whole IFM (frequency versus power) is achieved by extracting and combining the probe gains in all measurements. It should be mentioned that, the input signal is periodic and one period is measured in each step. In order to measure the non-repetitive signal, possible solutions can be considered such as the use of fiber loops for signal buffering [24], which is now under study.

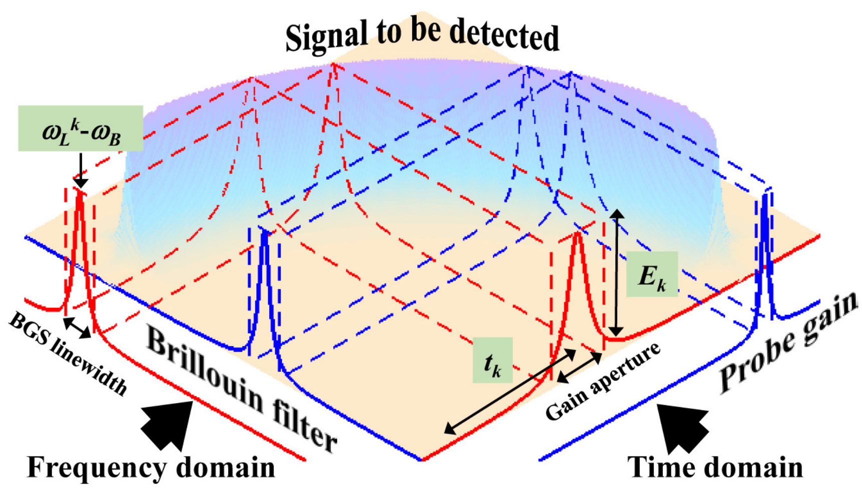

Fig. 2. Illustration of the spectral and temporal resolution of the SBS based IFM. Through tuning the pump frequency, the Brillouin filters with different frequency center affect the corresponding components along the signal. The spectral resolution is dependent on the BGS linewidth and the temporal resolution is related to the signal's characterization.

Figure 2 gives an example to illustrate the broadband IFM and its resolution. The 3D surface describes the instantaneous spectrum of the signal and two specific cases with different ω_L that are printed in red and blue, respectively. In the k-th step measurement, the signal is processed by the Brillouin filter with the intrinsic Brillouin linewidth at a certain frequency center of ω_L^k-ω_B. The probe gain profiles denote the processed results. The IFM spectral resolution is dependent on the BGS linewidth and the temporal resolution is decided by the time aperture of the probe gain. According to Eq. (1), the linewidth of the BGS is inverse to τ_p, which is usually considered to be 30 MHz in a single-mode optical fiber. Moreover, the Brillouin filter linewidth depends on the pump power and narrows on increasing the pump power for gain resonance [25,26]. It may improve the spectral resolution, which is under the future study. On the other hand, the gain apertures of the probe gains may

Optics EXPRESS

vary for different slope of the signal's frequency changing. As a result, the temporal resolution is dependent both on the phonon lifetime and the signal itself.

The system's bandwidth denoted by B_M is limited by the electro-optic modulator, which is used to modulate the microwave signal or to tune the pump frequency. If the modulated frequency is out of this bandwidth, the amplitude inhomogeneity and power loss will seriously influence the power measurement. Note that ω_L should be higher than the designed filtered frequency by ω_B, as schematically illustrated in the inset of the Fig. 3. There are several cases of choosing the sideband of the modulations for pump and probe lightwaves, as shown in Figs. 3(a)–3(d). If the upper sidebands are selected for both pump and probe lightwaves, when the signal's frequency is close to B_M, the pump lightwave will be out of range of the modulator [see Fig. 3(a)]. In this way the system's IFM range is $B_M - \omega_B$. Choosing the lower sidebands for the pump and probe lightwaves can avoid this problem [see Fig. 3(b)], which makes the measurement range reach B_M as it is limited by the modulator for probe lightwave. However, when the microwave signal's frequency is around ω_B [see Fig. 3(c)], the pump's sideband gets close to its carrier (i.e. laser source). This situation is nominated the carrier effect. For this effect, the detected Brillouin gain is contributed by not only the pump itself (generated by the sideband of the SSBM1 in Fig. 4) but also by the laser source itself (i.e. the carrier). Moreover, the modulation efficiency of the SSBMs in this study is not high for low input frequencies. Consequently, the power measurement for this effect is not just due to the SBS process, which becomes less reliable. In principle, if the upper sidebands of SSBMs were used for both the pump and probe lightwaves [see Fig. 3(d)], this effect might be overcome. However, since $2\omega_B$ should be smaller than B_M, much broader bandwidth of SSBMs turns to be necessary. It should be noted that the influence of the BFS in the fiber might be overcome if two individual lasers are used for pump and probe lightwaves. However, the system's bandwidth is still limited by the modulator for modulating the signal to be analyzed. Besides, two individual lasers may bring in additional frequency errors.

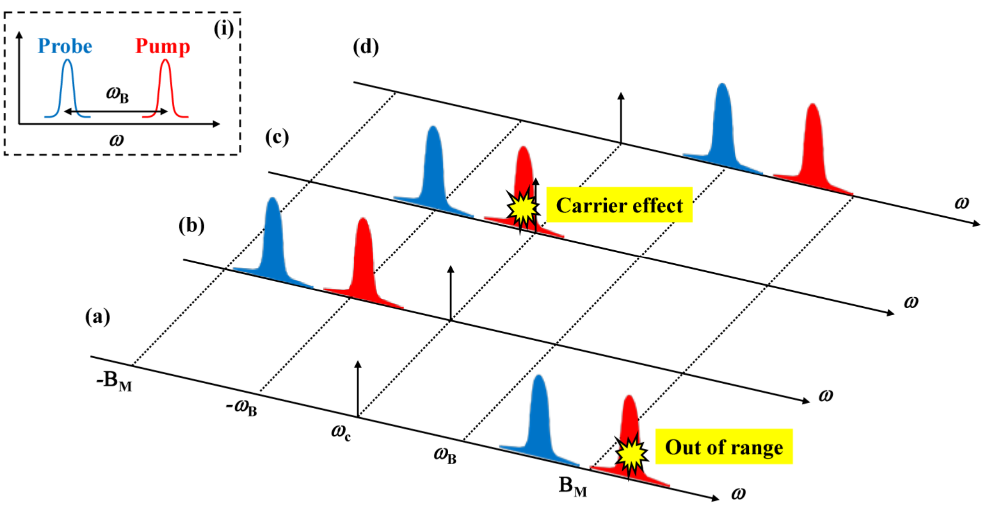

Fig. 3. Several cases of the sidebands management. (a) Both upper sidebands: signal's frequency is limited to $B_M - \omega_B$. (b) Lower sideband for probe: measurement range can reach B_M. When probe frequency is close to ω_B, (c) lower sidebands for probe suffer the carrier whereas (d) upper sidebands don't. The inset (i) schematically shows the relation between pump and probe lightwaves in frequency domain.

3. Experimental details

Figure 4 depicts the experimental setup. A 1550 nm distributed-feedback laser (DFB-LD, NEL NLK1C6DAAA) is split into two paths by a 50:50 fiber coupler. The upper branch

Optics EXPRESS

serving as the pump lightwave is modulated by a single sideband modulator (SSBM1) with the bandwidth of 20 GHz to generate the frequency shift between these two branches. The lower branch works as the probe lightwave. Through another SSBM2 with the bandwidth of 20 GHz, the probe lightwave is modulated by the input microwave signal to be measured. Both the pump and probe branches are modulated at the carrier-suppressed single-sideband modulation state with the sideband suppression ratio of 20 dB. The RF signal for SSBM1 is controlled to ensure that the unknown signal interacts with the pump lightwave with single frequency in each-step measurement. The first lower/higher sideband of the modulated lightwaves after SSBM1 is selected and thus the beating between the pump and probe is close to the BFS of the optical fiber, which is 10.743 GHz in the experiment. Polarization controllers (PC1 and PC2) are used to optimize the light polarizations before the modulators. Erbium-doped fiber amplifiers (EDFA1 and EDFA2) are utilized to compensate and control the optical power of the pump and probe lightwaves. The injected powers of pump and probe lights into the fiber are around 22 dBm and 17 dBm, respectively. PC3 and PC4 are used to maximize the SBS interaction in a 200-meter standard single-mode optical fiber (SMF). A circulator is used for the isolation and transmission of the amplified probe lightwave. A photo-detector (PD) with the bandwidth of 1 GHz converts the detected probe power into the electric voltage, which is sampled by an oscilloscope (Tektronix, DSA70804) with the sampling rate of 1.25 GS/s. An attenuator is used to prevent the saturation of the PD and the optical power launched into the PD is −3 dBm.

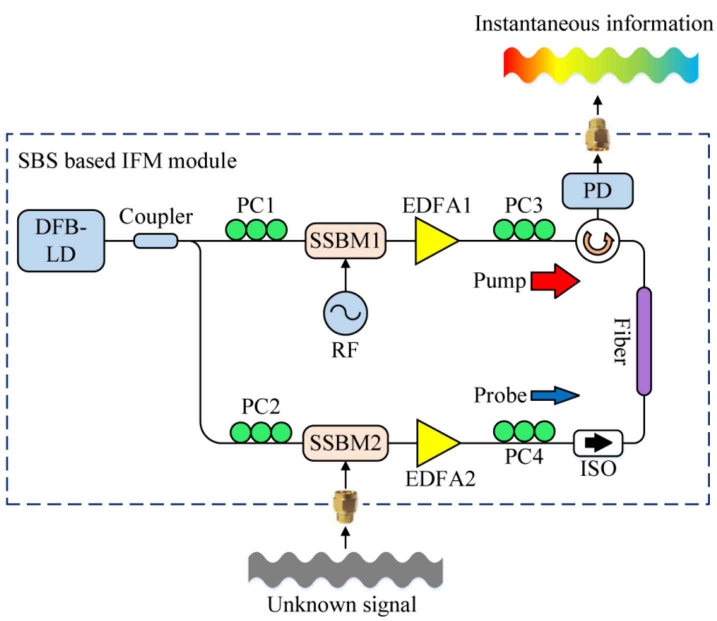

Fig. 4. Experimental setup. DFB-LD: distributed-feedback laser. PC: polarization controller. SSBM: single sideband modulator. EDFA: erbium-doped fiber amplifier. ISO: isolator. PD: photo-detector.

Proof-of-concept experiments are carried out to verify the feasibility of this scheme. An LFM pulse with the 4.3-5.3 GHz frequency range and 1 μs period is generated by a voltage-controlled oscillator (VCO, Mini-circuits ZX95-5400-S +). The measured results are shown in Fig. 5. First, the LFM pulse is digitally sampled by the oscilloscope with 25 GS/s sampling rate and 8 GHz bandwidth. Its short-time Fourier transform result is given in Fig. 5(a). Second, the probe gain under each pump frequency condition is successively recorded by the oscilloscope, which is combined together and thus depicted in Fig. 5(b). Note that the sampling rate and bandwidth in Fig. 5(b) are only 1.25 GS/s and 1 GHz, respectively. The

Optics EXPRESS

reason of the lower sampling rate and bandwidth is because the digital way processes the signal itself whereas the SBS based IFM deals with its probe gain. By searching the maximum frequency at each moment in Figs. 5(a) and 5(b), the curves that describe frequencies changing with time are plotted in Fig. 5(c) for comparison. SBS measured result matches well with the digital one and their differences are summarized in Fig. 5(d). It can be seen that all the detection errors are within 20 MHz, which verifies the spectral resolution we analyzed above.

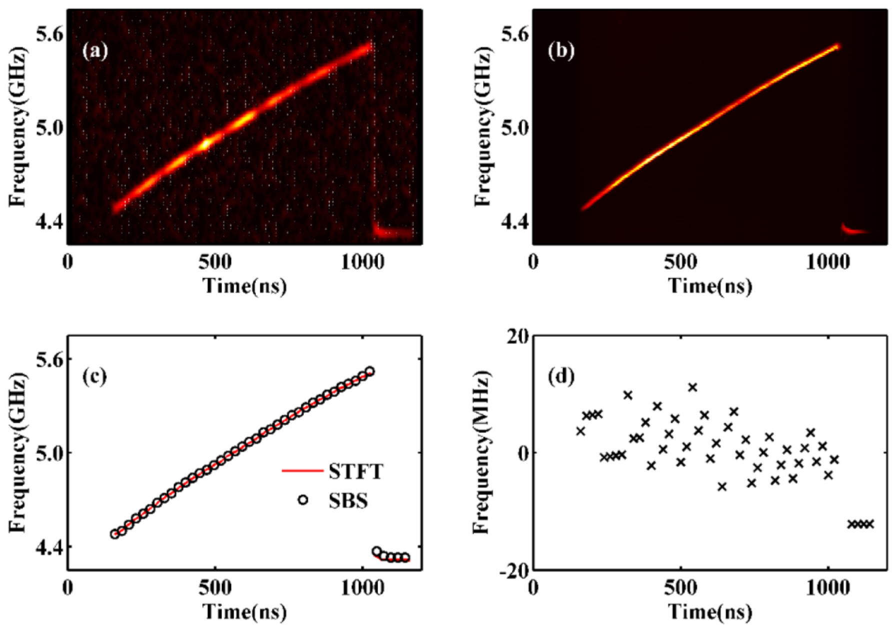

Fig. 5. Proof-of-concept experimental result for an LFM pulse with 1 μs duration and 1 GHz sweep range (from 4.3 GHz to 5.3 GHz). (a) Short-time Fourier transform result based on direct sampling/processing. (b) Combined probe gain from the SBS based IFM. (c) Comparison between two IFM calculated from (a) and (b). (d) Measured frequency errors.

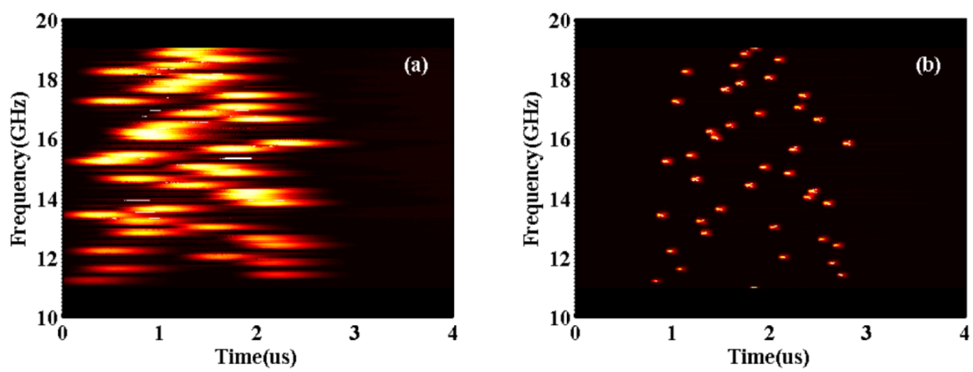

Fig. 6. Measurement results for the frequency Costas coded pulses. The frequency step is 200 MHz. The time steps are (a) 5 ns and (b) 50 ns, respectively.

Another type of waveform, the frequency Costas coded pulse [27], is employed for the further measurement. The experimental setup is the same as the previous LFM pulse measurement. Two pulses with both spectral range from 11 GHz to 19 GHz and 2 μs duration are used. The frequency steps of both pulses are 200 MHz and the time steps are set to be 5 ns and 50 ns, respectively. Figure 6 shows the combined probe gain measured from these two

Optics EXPRESS

waveforms. It is found that Fig. 6(b) is more explicit that Fig. 6(a). This is because 5 ns time step is much shorter than the phonon lifetime of around 10 ns.

In order to verify the ability of the broadband IFM, we measure another LFM pulse with 1 μs duration and 27.5 GHz frequency range sweeping from 0.5 GHz to 28 GHz. The whole measurement is divided into two parts: one part is scanned from 0 to 12 GHz and the other part from 12 GHz to 29 GHz. In the first part, two measurement results obtained with upper or lower sideband of the modulation for the probe lightwave are given in Figs. 7(a) and 7(b), respectively. When choosing the upper sideband [see Fig. 7(a)], the detected power grows weak with the frequency going high. This is because the pump frequency has to exceed 20 GHz, which is the bandwidth of the modulator used in this study. Meanwhile, using lower sideband dose not suffer this power attenuation [see Fig. 7(b)]. In the second part, it can be only detected by the lower sideband case (both for pump and probe) in our experiment, even though the signal's frequency exceeds 20 GHz as well. Combined with Fig. 7(b), the whole range measurement result is depicted in Fig. 7(c).

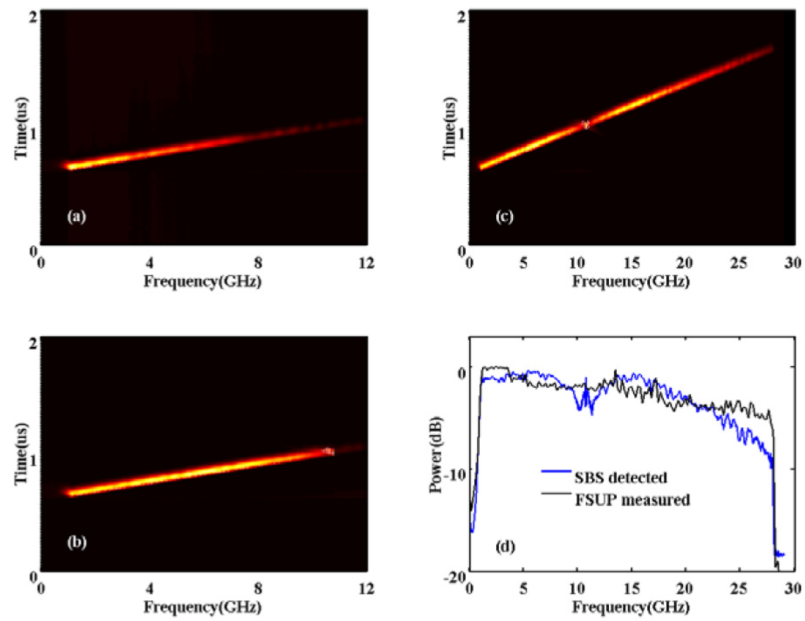

Fig. 7. Experimental results for an LFM signal with frequency sweeping from 0.5 GHz to 28 GHz. The entire measurement is divided into two parts. One part scanned from 0 to 12 GHz is implemented with (a) upper sideband modulation or (b) lower sideband modulation for the probe lightwave. (c) The entire measurement result. (d) The power spectrum of the signal by searching the peak values of (c) is compared to the spectrum measured by the FSUP.

Through searching the peak values in Fig. 7(c), the power spectrum of the broadband signal is illustrated in Fig. 7(d). It is compared with the electrical power spectrum that is measured by a signal source analyzer (Rohde&Schwarz, FSUP) with the bandwidth of 50 GHz. Both these two power spectrums are normalized as the strongest powers. The power spectrum measured by the SBS process shows somehow attenuations in two regions. One appears around 10 GHz is due to the carrier effect as explained in Fig. 3. It should be noted that the choice of upper sidebands of SSBMs to overcome this effect is limited by the experimental devices. The other occurs beyond 20 GHz. Since B_M of the modulator for the probe branch is 20 GHz, the insufficient modulation efficiency weakens detected power. Although the compared power spectra are normalized, this proposed scheme is potentially able to detect the absolute amplitude in principle. The relation between the Brillouin gain and the signal's amplitude is affected by several factors including fiber length, additional

Optics EXPRESS

amplification/attenuation, and the modulation/detection efficiency. If these factors are further analyzed, it is expected to obtain the absolute instantaneous power.

4. Conclusion

We have demonstrated a newly proposed broadband IFM scheme based on SBS process. Narrow linewidth of SBS process is utilized to detect the instantaneous spectrum information of the microwave signal that is modulated onto the probe lightwave. Through tuning the frequency of the counter-propagating pump lightwave, the instantaneous information is extracted and obtained by detecting the probe gain. Spectral resolution is decided by the linewidth of the BGS whereas the temporal resolution is dependent on the phonon lifetime. The IFM bandwidth is mainly determined by the bandwidth of the electro-optic modulator. Through sideband management of the two SSBMs, the BFS of the optical fiber doesn't limit the IFM bandwidth. Experiments on LFM pulses and frequency Costas coded pulses have been carried out to verify the feasibility of this scheme with the frequency errors of 20 MHz and the broadband of 27.5 GHz.

Funding

National Natural Science Foundation of China (61571292 and 61535006); SRFDP of MOE (20130073130005).